

Kinetic Study of Decolorization of Methylene Blue with Sodium Sulphite in Aqueous Media: Influence of Transition Metal Ions

Olajire AA* and Olajide AJ

Industrial and Environmental Chemistry unit, Department of Pure and Applied Chemistry, Ladake Akintola University of Technology, Ogbomoso, Nigeria

Abstract

The kinetics of decolorization of methylene blue (MB⁺) with sodium sulphite in aqueous media was investigated over the temperature range 20-40°C. The kinetic studies were carried out as a function of different variables like concentration, pH, and temperature on rate of decolorization. The rate of the reaction was found to be [H⁺] dependent and first order in both [MB⁺] and reductant. The empirical rate law conforms to the equation:

$$\frac{d[MB^+]}{dt} = -\{k_3 + k_2K_1[H^+]\} [MB^+][SO_3^{2-}] = -k_{obs} [MB^+]$$

Where K_1 is the protonation constant, and k_2 and k_3 are overall pseudo-second order rate constants for the decolorization of MB⁺ with SO_3^{2-} . The rate was found to increase linearly with temperature. The rate of decolorization decreased after addition of Co(II), Ni(II), Mn(II) and Zn(II), but increased after addition of Fe(II) and Cu(II). The activation parameters (E_a , ΔG^\ddagger , ΔH^\ddagger and ΔS^\ddagger) of the decolorization reaction of MB⁺ with SO_3^{2-} in absence and in presence of Fe(II) and Cu(II) were calculated.

Keywords: Methylene blue; Sodium sulphite; Metal activation; Kinetics; Decolorization

Introduction

A variety of hazardous pollutants are discharged into the aquatic bodies from several industrial streams [1,2]. Dye from textile industries and other commercial dyestuffs have been a focus of environmental remediation in the last few years [1,3,4]. The use of methylene blue as a dye in textile industry [5] has decreased slightly in last few years due to its high light sensitivity. However, it is still widely used for the manufacture of color pens and polygraphic inks [6]. The color and toxicity which dyes impart to water bodies are very undesirable and harmful to the water users for aesthetic and environmental reasons [7,8].

Methylene blue (MB) is a cationic dye, used extensively for dyeing cotton, wool and silk. The risk of the existence of this dye in waste water may be arisen from the burns effect of eye, nausea, vomiting and diarrhea [9,10]. Generally, several methods have been developed for the removal of dyes from effluents including precipitation, adsorption, and reverse osmosis, aerobic and anaerobic treatment, oxidation and reduction [11-19]. To find a general process for treatment of the color of dye used in dyeing processes is very difficult due to the complexity and variety of these types of industrial wastewater. The disadvantages of these methods are sludge formation, waste disposal and high operation cost, time consuming and ineffectiveness in cases where complicated aromatic compounds are present [20,21].

Literature is rich in articles about kinetic studies of the oxidation of MB⁺. Studies on redox reaction of methylene blue are mainly focused on the kinetics of transformation into leuco-MB [22,23], whereas the kinetics of its reductive decolorization in the presence of transition

metal ions have been very scanty. The decolorization can be obtained by SCN⁻ (partial decolorization) [24], H₂O₂ [25,26], UV/H₂O₂ [27,28], ascorbic acid [29-32], strong oxidant such Ce (IV) [33], KBrO₃ [34,35], KClO₃ [36], O₃ [37], UV/O₃ [38], activated O₂ [39], Fenton's reagent [40-42], photo Fenton [43], persulfate [44], photodecomposition on TiO₂ [45,46], Br₂ in basic medium [47], sulphide (Na₂S) [48], and finally, reducing sugar [49]. Sulphite which sometime plays the role of oxidant and sometimes the role of a reductant, is employed in this study. The preliminary test showed the addition of sulphite (Na₂SO₃) in excess to a MB⁺ solution faded its blue color with time, and therefore interesting to deeply study the kinetics and parameters affecting this decolorization. Also investigated, is whether the addition of small amount of transition metal ions influence decolorization rate of methylene blue with sulphite. The red-ox properties of methylene blue make a useful indicator in analytical chemistry [50]. Methylene blue is blue when it is in an oxidizing environment, but colorless (leuco methylene blue (LMB)) if it is exposed to a reducing agent (Scheme 1).

These processes have found applications in numerous inventions like data recording holographic industries, optical data storage, food and pharmaceutical industries. Such reduction is also used in checking the purity of milk [51,52].

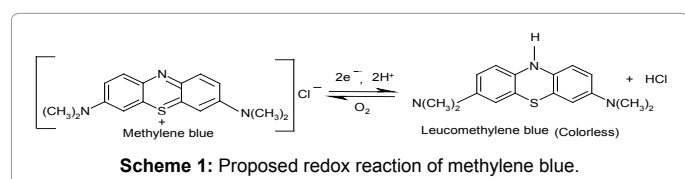
In the present study, an attempt is made to investigate the decolorization kinetics of methylene blue with sodium sulphite in aqueous media by UV-Visible spectrophotometry. The effect of various parameters such as initial pH, initial concentration of sulphite, MB⁺ and transition metal ions concentration was studied.

*Corresponding author: Olajire AA, Industrial and Environmental Chemistry unit, Department of Pure and Applied Chemistry, Ladake Akintola University of Technology, Ogbomoso, Nigeria, Tel: 2348033824264; E-mail: olajireaa@yahoo.com

Received April 04, 2014; Accepted April 28, 2014; Published April 30, 2014

Citation: Olajire AA, Olajide AJ (2014) Kinetic Study of Decolorization of Methylene Blue with Sodium Sulphite in Aqueous Media: Influence of Transition Metal Ions. J Phys Chem Biophys 4: 136. doi:10.4172/2161-0398.1000136

Copyright: © 2014 Olajire AA, et al. This is an open-access article distributed under the terms of the Creative Commons Attribution License, which permits unrestricted use, distribution, and reproduction in any medium, provided the original author and source are credited.



Experimental Procedure

All chemical reagents used were of analytical grade. Methylene blue was obtained from M & B Laboratory Chemicals in the laboratory grade and used without further purification. Distilled water was used to prepare all solutions. A stock solution of Na_2SO_3 and MB^+ were prepared by dissolving the required amount in distilled water. A Na_2SO_4 solution was added to reaction mixture in order to maintain the ionic strength of the solution. The effect of pH was also studied by adjustment of pH of the reaction mixture prior to decolorization with NaOH or HCl and measured by a pH meter (JENWAY 3505 pH meter). The effect of temperature was studied and the temperature was controlled by a horizontal thermostated shaker (SM 101 by Surgafriend Medicals). The absorbance of the reaction mixture at different reaction times was recorded by measuring the absorption intensity at 661nm (λ_{max} of MB^+) using Genesys 10 UV-VIS Scanning Spectrophotometer. The reaction mixtures were allowed to undergo complete reaction as evident from the constancy of repeated measurements of absorbance (A_∞) at 661 nm. The concentration at any time t (C_t) was obtained from the difference in the absorbance at time t (A_t) and at infinity (A_∞).

$$C_t = A_t - A_\infty \quad (1)$$

The efficiency of MB^+ decolorization was calculated by using Equation 2:

$$\text{Degradation efficiency} = \frac{C_o - C_t}{C_o} \times 100\% = \frac{A_o - A_t}{A_o} \times 100\% \quad (2)$$

Where, C_o and C_t are MB^+ concentration at initial and any time

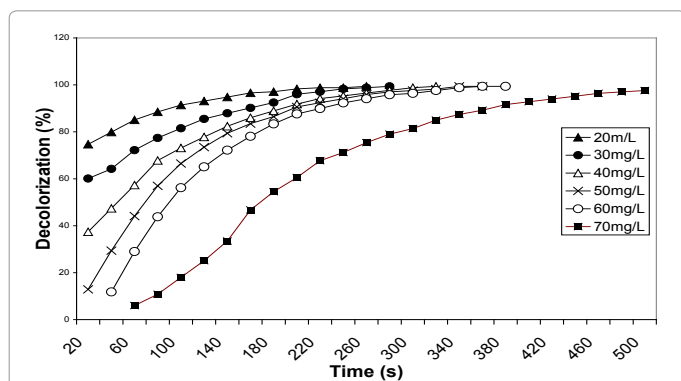


Figure 1: Time profile of MB^+ decolorization with Na_2SO_3 at varying initial MB^+ concentrations. Time profile of MB^+ decolorization with Na_2SO_3 at varying initial MB^+ concentrations.

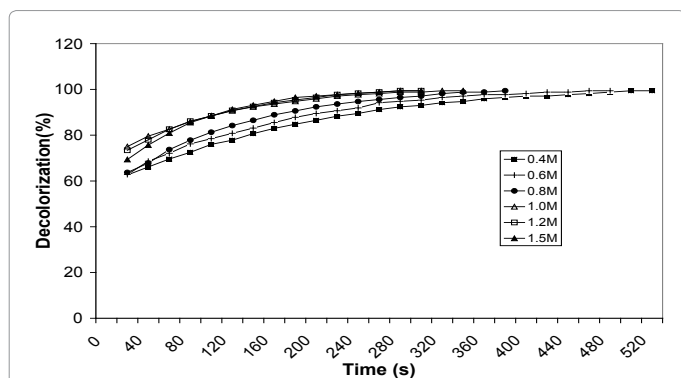


Figure 2: Time profile of MB^+ decolorization with Na_2SO_3 at varying initial Na_2SO_3 concentrations.

respectively. The parameters A_o and A_t are the absorbance of the MB^+ solutions in the 661nm wavelength at initial and any time respectively.

The effects of transition metal ions was investigated by adding various concentrations of transition metal solutions ($\text{CoCl}_2 \cdot 6\text{H}_2\text{O}$, $\text{NiCl}_2 \cdot 6\text{H}_2\text{O}$, $\text{CuSO}_4 \cdot 5\text{H}_2\text{O}$, ZnCl_2 , $\text{FeSO}_4 \cdot 7\text{H}_2\text{O}$ and $\text{MnCl}_2 \cdot 4\text{H}_2\text{O}$) in the range 0.1 – 0.5 mg/dm^3 at 30°C with fixed amounts of MB^+ (20 mg/dm^3) and Na_2SO_3 (1.0 mol/dm^3).

Results and Discussion

Effect of initial concentration of MB^+

The extent of MB^+ decolorization by Na_2SO_3 with time at varying initial MB^+ concentrations (20–70 mg/dm^3) under identical conditions is shown in Figure 1. It is seen that the decolorization of MB^+ is relatively fast at the beginning and decreases as the reaction progresses. At low concentration (20 mg/dm^3), MB^+ is almost completely decolorized by Na_2SO_3 within 60 s., which is also evident from the absorbance data recorded with reaction time (Figure 1a). The time profiles of MB decolorization show that the decolorization is substantially decreased with increase in initial MB^+ concentration. For example, the extent of decolorization after 60 s decreases from 85% to 29% with increase in concentration of MB^+ from 20 to 70 mg/dm^3 with Na_2SO_3 .

Effect of initial concentration of SO_3^{2-}

The effect of Na_2SO_3 on the decolorization of MB^+ was investigated by varying initial concentration of Na_2SO_3 from 0.4 to 1.5 mol/dm^3 , the results are shown in Figure 2. It was observed that the decolorization efficiency increases from 69.6% to 80.9% as a consequence of increasing Na_2SO_3 concentration from 0.4 to 1.5 mol/dm^3 within 60 sec. This is due to increasing reductive power of the sulphite. The maximum decolorization efficiency of about 99.4% was achieved with 1.5 mol/dm^3 of Na_2SO_3 within 5 min.

Kinetic study

The reductive decolorization of MB^+ by sulphite was a complicated process probably due to various reduced forms of MB^+ [22]. The process could not easily be depicted by simple reaction kinetics. To estimate the kinetics rate of decolorization, an equation form of power law is used:

$$-\frac{d[C]}{dt} = k[\text{SO}_3^{2-}]^n [C]^m \quad (3)$$

where k is the removal rate constant, $[C]$ is the MB^+ concentration, m and n are the pseudo order of reaction with respect to MB^+ and SO_3^{2-} respectively. The rate equation can be stated with observed rate constant (k_{obs}) as follows:

$$-\frac{d[C]}{dt} = k_{\text{obs}} [C]^m \quad (4) \text{ and } (5)$$

where,

$$k_{\text{obs}} = k[\text{SO}_3^{2-}]^n$$

For a zero-order reaction, the above equation after integration becomes:

$$C_t = k_o t \quad (6)$$

Also for a first-order reaction, the above equation after integration becomes:

$$\ln(C_t) = \ln(C_o) - k_1 t \quad (7)$$

in which, C_o is the initial MB^+ concentration and C_t is the

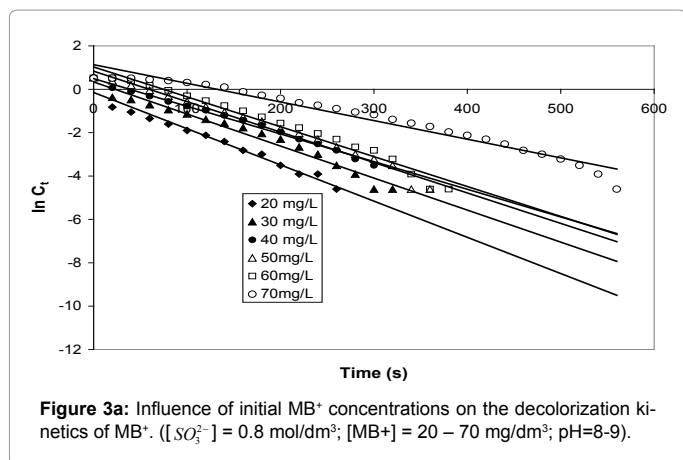


Figure 3a: Influence of initial MB⁺ concentrations on the decolorization kinetics of MB⁺. ([SO₃²⁻] = 0.8 mol/dm³; [MB⁺] = 20 – 70 mg/dm³; pH=8-9).

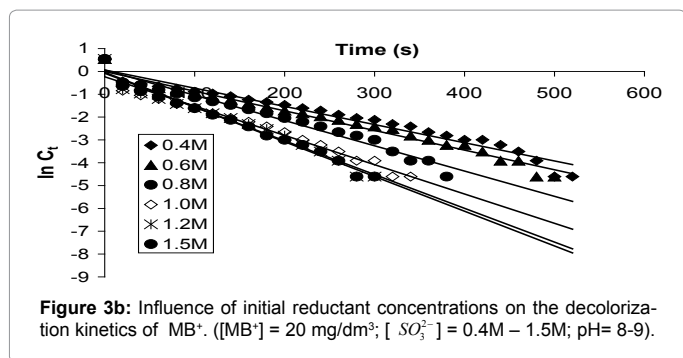


Figure 3b: Influence of initial reductant concentrations on the decolorization kinetics of MB⁺. ([MB⁺] = 20 mg/dm³; [SO₃²⁻] = 0.4M – 1.5M; pH= 8-9).

[SO ₃ ²⁻], mol dm ⁻³	Zero order		First order		Second order	
	k _o x 10 ⁻³	R ²	k ₁ x 10 ⁻³	R ²	k ₂ x 10 ⁻²	R ²
0.4	1.6	0.576	8.0	0.960	9.8	0.506
0.6	1.8	0.547	8.6	0.975	15.0	0.625
0.8	2.4	0.554	11.1	0.972	16.1	0.598
1.0	2.4	0.422	12.8	0.968	24.6	0.704
1.2	3.0	0.457	14.8	0.966	27.8	0.659
1.5	3.1	0.485	15.2	0.978	28.1	0.678
[MB ⁺] mg/L	Zero order		First order		Second order	
	k _o x 10 ⁻³	R ²	k ₁ x 10 ⁻²	R ²	k ₂ x 10 ⁻¹	R ²
20	3.6	0.452	1.67	0.968	2.81	0.705
30	3.6	0.634	1.48	0.972	2.78	0.629
40	3.8	0.764	1.28	0.993	1.73	0.550
50	4.2	0.802	1.40	0.978	1.96	0.528
60	4.5	0.832	1.38	0.972	1.89	0.533
70	3.3	0.890	0.86	0.962	0.81	0.449

Table 1: Kinetics rates of reaction with respect to MB⁺ and SO₃²⁻.

concentration at reaction time *t*. For a second-order reaction, the integrated equation becomes:

$$\frac{1}{C_t} = \frac{1}{C_o} + k_2 t \quad (8)$$

The absorbance-time data plot of the above reaction orders were carried out to determine the rate constant, *k_{obs}* and best order for the reaction process. The zero-, first- and second-order kinetics rate constants for the decolorization of MB⁺ with SO₃²⁻ were obtained from the plots, and the results were shown in Table 2. It was observed that the correlation coefficients for the three models are different. The first-order kinetics shows highest correlation (*R*²>0.9) than both zero and second-order kinetics (*R*²<0.9). It can therefore be concluded that the decolorization of MB⁺ with SO₃²⁻ fits the first-order reaction kinetics of the type:

$$\ln \frac{C_t}{C_o} = -k_1 t \quad (9)$$

From the pseudo first-order kinetic plots (Figures 3a and 3b), the pseudo-first order rate constants with respect to MB⁺ and SO₃²⁻ were obtained (Table 1).

The pseudo first-order rate constant decreased with increasing initial concentration of methylene blue (Figure 4a). The possible explanation is that at high dye concentrations, the reductive activity of sulphite might be reduced due to coverage of reducing ion species by the dye ions.

Similarly, the pseudo first-order rate constant increased with increasing concentration of SO₃²⁻. The explanation for this trend is that at high sulphite concentration, there is high concentration of reducing ion species which override the coverage effect of the dye ions. The plot of *k_{obs}* versus sulphite concentration ranging from 0.4-1.5 mol dm⁻³ shows a linear relationship between *k_{obs}* and [SO₃²⁻] (Figure 4b). This fact reveals also first-order dependence on the reductant. An overall rate equation can then be explained in the form:

$$-\frac{d[MB^+]}{dt} = k_{obs}[MB^+] = k_2[SO_3^{2-}][MB^+] \quad (10)$$

where *k₂* is the overall second order rate constant.

$$k_2 = \frac{k_{obs}}{[SO_3^{2-}]} \quad (11)$$

Effect of pH

In view of the fact that pH of dye solution is a main parameter on the decolorization progress, the experiments were carried out to

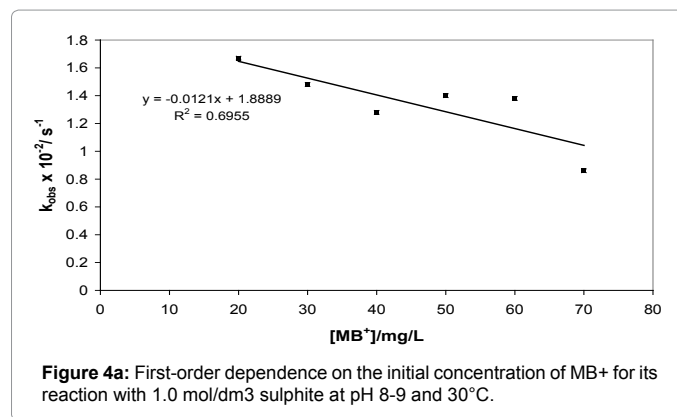


Figure 4a: First-order dependence on the initial concentration of MB⁺ for its reaction with 1.0 mol/dm³ sulphite at pH 8-9 and 30°C.

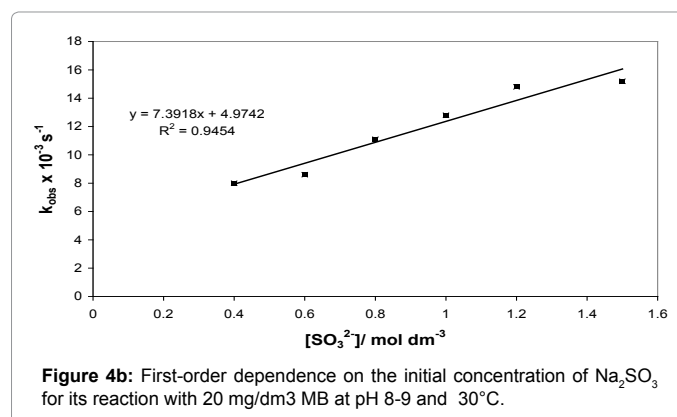


Figure 4b: First-order dependence on the initial concentration of Na₂SO₃ for its reaction with 20 mg/dm³ MB at pH 8-9 and 30°C.

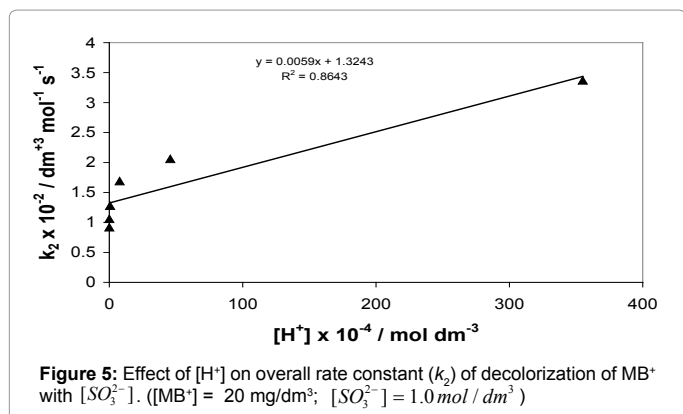


Figure 5: Effect of $[H^+]$ on overall rate constant (k_2) of decolorization of MB^+ with $[SO_3^{2-}]$. ($[MB^+] = 20 \text{ mg/dm}^3$; $[SO_3^{2-}] = 1.0 \text{ mol/dm}^3$)

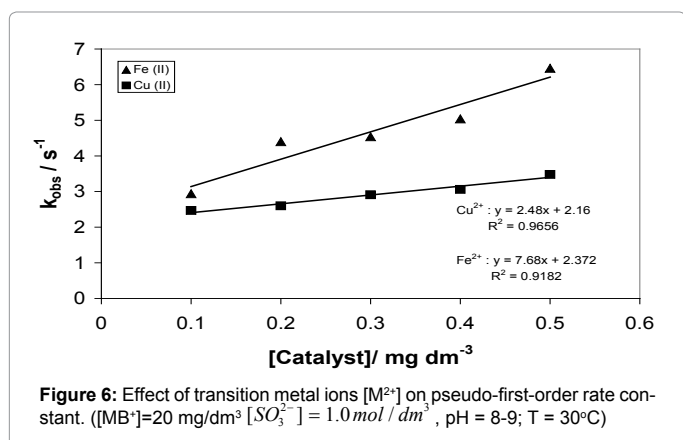


Figure 6: Effect of transition metal ions $[M^{2+}]$ on pseudo-first-order rate constant. ($[MB^+] = 20 \text{ mg/dm}^3$; $[SO_3^{2-}] = 1.0 \text{ mol/dm}^3$, pH = 8-9; T = 30°C)

$[M^{2+}] / \text{mg dm}^{-3}$	Cu^{2+}	Fe^{2+}	Zn^{2+}	$k_{obs} \times 10^{-2} / s^{-1}$	Mn^{2+}	Co^{2+}	Ni^{2+}
0.1	1.03	2.94	1.24	1.32	1.37	0.63	
0.2	1.05	4.40	1.28	1.42	1.45	0.95	
0.3	1.12	4.54	1.55	1.43	1.39	1.08	
0.4	1.20	5.04	1.51	1.51	1.46	0.89	
0.5	1.45	6.46	1.51	1.45	1.11	1.04	

Table 2: Influence of transition metal ions on the rate of decolorization (k_{obs}) of MB^+ with SO_3^{2-} . ($[MB^+]_0 = 20 \text{ mg/dm}^3$; $[Na_2SO_3] = 1.0 \text{ mol/dm}^3$; pH = 8-9; T = 30°C)

find the optimal pH of reaction mixture for decolorization of MB^+ . The examined pH range was from 1-8, which was adjusted by using appropriate amounts of base (NaOH) or acid (HCl) solutions. It was observed that the decolorization of MB^+ was significantly influenced by the solution's pH values, and the highest decolorization rate (k_{obs}) was achieved at pH 1.45. These observations are in good agreement with published results [40,53-56].

The plot of k_2 versus $[H^+]$ was linear with a positive intercept. The acid dependent rate equations for the reactions can be represented by equation 12.

$$-\frac{d[MB^+]}{dt} = \{a + b[H^+]\}[MB^+][SO_3^{2-}] \quad (12)$$

$a = 1.32 \times 10^{-2} \text{ dm}^3 \text{ mol}^{-1} \text{ s}^{-1}$ and $b = 0.595 \text{ dm}^6 \text{ mol}^{-2} \text{ s}^{-1}$

The above equation (12) suggests that the reaction occurs via acid-dependent and acid-independent pathways. The high rate constant value observed at lower pH can be explained by the change in the MB^+ structure. The labile H atom makes the molecule of MB^+ dye vulnerable towards the attack of reductant. This has been explained in terms of

protonation of SO_3^{2-} in a fast step to give HSO_3^- which subsequently reacts with the substrate in a slow step to give the product [57].

Effect of transition metal ions

Different transition metal ions, Fe(II), Cu(II), Ni(II), Mn(II), Zn(II) and Co(II) were tested as a catalyst for the decolorization of MB^+ with SO_3^{2-} . The results show that Fe(II) and Cu(II) accelerate the reaction rate with varying catalytic activity (Figure 6), while others have no catalytic effect on the rate of reaction (Table 2). It was observed that the rate of reaction between methylene blue and sodium sulphite was increased by the presence of trace amounts of Fe (II) and Cu(II) ions. A plot of rate constant versus [Fe (II)] and [Cu (II)] gives a straight line with almost the same values of intercept of about 2.0 s^{-1} , which is equal to the rate of the uncatalyzed reaction. The values of slopes are quite different: 7.68 and $2.48 \text{ dm}^3 \text{ mg}^{-1} \text{ s}^{-1}$ for Fe(II) and Cu(II) respectively.

The rate constant in the presence of Fe^{2+} and Cu^{2+} ions is greater than in the absence of these transition metal ions. This could be due to activation of sodium sulphite by these transition metal ions to produce sulphate anion radical ($SO_4^{\bullet-}$) via sulfite radical anion [58-60]. The sulfite can be oxidized to sulphate by trace transition metal ions via free radicals. This metal-catalyzed autoxidation generates sulfur trioxide anion radical ($SO_3^{\bullet-}$) in an initiating one-electron oxidation step through an oxygen-consuming chain reaction [61-64] in accordance with the following reaction scheme 2.

Effect of temperature

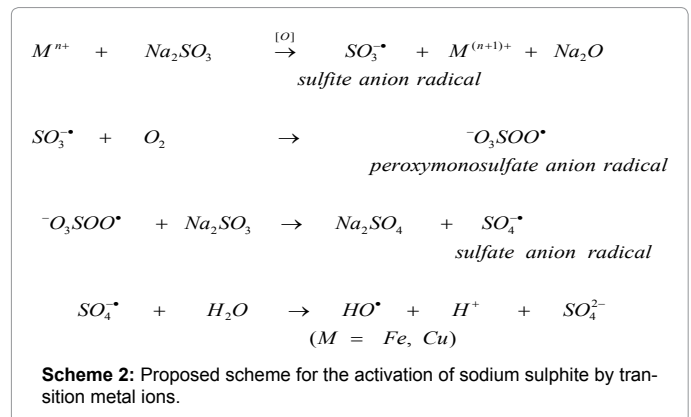
The effect of temperature on decolorization of methylene blue in the presence and absence of transition metal ions catalyst was investigated in the range of 293-313 K. The results in Figure 7 show that the decolorization efficiency of methylene blue gradually increased with increase in the temperature. The increase in temperature may lead to increasing reduction rate of methylene blue.

The activation parameters associated with the decolorization of methylene blue are calculated from the plot of $\ln k_{obs}$ versus $1/T$ (Figure 7), which gives the value of activation energy (E_a), according to the Arrhenius equation:

$$\ln k_{obs} = \frac{-E_a}{RT} + \ln A \quad (13)$$

The values of ΔH^\ddagger and ΔS^\ddagger can be calculated from the plot of the Eyring equation [65] as follows:

$$\ln(k_{obs}/T) = \left(\ln \frac{k_B}{h} + \frac{\Delta S^\ddagger}{R}\right) - \frac{\Delta H^\ddagger}{RT} \quad (14)$$



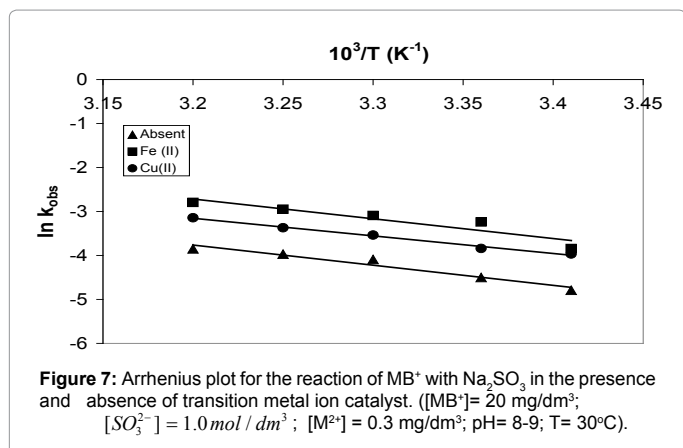


Figure 7: Arrhenius plot for the reaction of MB⁺ with Na₂SO₃ in the presence and absence of transition metal ion catalyst. ([MB⁺]=20 mg/dm³; [SO₃²⁻]=1.0 mol/dm³; [M²⁺]=0.3 mg/dm³; pH=8-9; T=30°C).

T (°C)	k _{obs} × 10 ⁻² / s ⁻¹			E _a / kJ mol ⁻¹		
	Absent	Fe ²⁺	Cu ²⁺	Absent	Fe ²⁺	Cu ²⁺
20	0.83	2.14	1.89			
25	1.11	3.92	2.15			
30	1.67	4.54	2.91	38.13	37.42	33.33
35	1.89	5.24	3.44			
40	2.13	6.11	4.32			

Table 3: Rate constants and activation parameters for interaction of MB⁺ and SO₃²⁻ in the presence of catalyst. ([MB⁺]=20 mg/L; [SO₃²⁻]=1.0 mol/dm³; [Catalyst]=0.3 mg/dm³; pH=8-9; T=30°C).

M ²⁺	ΔH [#] / kJ mol ⁻¹	ΔS [#] / kJ mol ⁻¹ K ⁻¹	ΔG _{298K} [#] / kJ mol ⁻¹
Absent	35.56	-0.162	84.13
Fe ²⁺	34.83	-0.156	81.32
Cu ²⁺	30.78	-0.173	82.33

Table 4: Thermodynamic parameters for the reaction between MB⁺ and SO₃²⁻. ([MB⁺]=20 mg/dm³; [SO₃²⁻]=1.0 mol/dm³; [Catalyst]=0.3 mg/dm³; pH=8-9; T=30°C).

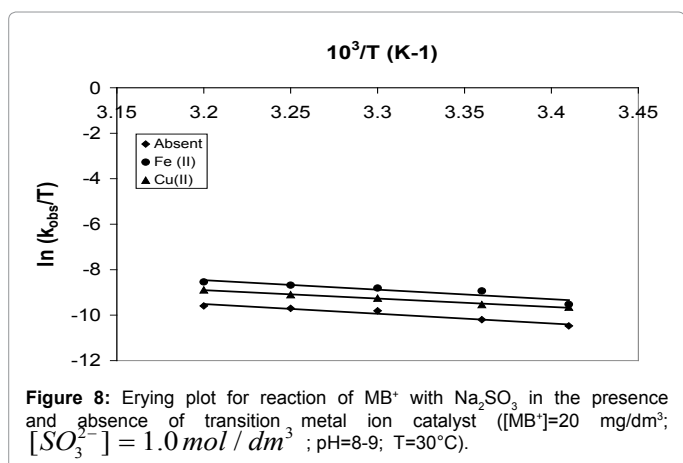


Figure 8: Eyring plot for reaction of MB⁺ with Na₂SO₃ in the presence and absence of transition metal ion catalyst ([MB⁺]=20 mg/dm³; [SO₃²⁻]=1.0 mol/dm³; pH=8-9; T=30°C).

Where, k_B is the Boltzmann's constant (1.381×10^{-23} J K⁻¹); h is the Planck's constant (6.626×10^{-34} J s), where $\ln \frac{k_B}{h} = 23.76$.

From the linear plot of $\ln(k_{obs}/T)$ versus $1/T$ (Figure 7), values of ΔH^\ddagger and ΔS^\ddagger can be calculated. The Gibbs' free energy ΔG^\ddagger can therefore be calculated from the relation:

$$\Delta G^\ddagger = \Delta H^\ddagger - T \Delta S^\ddagger \quad (15)$$

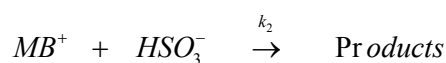
The rate constants and activation energies in the range of temperature studied (20-40°C) are listed in Table 3 while other

thermodynamic parameters are given in Table 4. The positive values of ΔG^\ddagger for the reaction (Table 4) indicate the non-spontaneous nature of decolorization of MB⁺ by sulphite at the temperatures studied. The negative value of ΔS^\ddagger suggest the decreased randomness at the liquid/liquid solution interface during the decolorization of MB⁺ solution by sulphite ion while the positive values of ΔH^\ddagger show the endothermic nature of the reaction.

The activation energy in presence of Fe(II) and Cu(II) is lower than in its absence (Table 3). The decrease in the activation energy (E_a) in presence of these transition metal ions confirms their catalytic effects (metal activation).

Reaction mechanism

Based on the above experimental findings and observations, the reaction mechanism has been suggested utilizing the redox properties of Na₂SO₃. It has also been noted that redox reactions of many oxyanions are strongly acid dependent [66]. Under the present experimental conditions, it is reasonable to postulate that SO₃²⁻ is protonated in a fast step to give HSO₃⁻ which then reacts with MB⁺ in a slow step to give the products [56]. Also, the intercept obtained from the plot of k_2 versus [H⁺] (Figure 5) indicates that the unprotonated SO₃²⁻ also reacts with MB⁺ to form the products. Therefore, taking recourse to the experimental data, the following mechanistic steps have been postulated for the reaction:



From equation (16)

$$\text{Rate} = k_2 [MB^+] [HSO_3^-] + k_3 [MB^+] [SO_3^{2-}] \quad (20)$$

Putting equation (20) into (19);

$$\text{Rate} = k_2 K_1 [MB^+] [SO_3^{2-}] [H^+] + k_3 [MB^+] [SO_3^{2-}] \quad (21 \text{ and } 22)$$

$$\text{Rate} = (k_3 + k_2 K_1 [H^+]) [MB^+] [SO_3^{2-}] = k_{obs} [MB^+]$$

where K_1 is the protonation constant, and k_2 and k_3 are the pseudo-second order rate constants for the protonation and deprotonation of MB⁺. Equation (22) shows acid dependence on the rate of decolorization of methylene blue with sodium sulphite and is similar to equation (12) with $k_3 = a' = 1.32 \times 10^{-2}$ dm³ mol⁻¹ s⁻¹ and $k_2 K_1 = b' = 0.595$ dm⁶ mol⁻² s⁻¹.

Conclusion

The color removal of the cationic dye methylene blue by the formation of a reduced form of MB⁺ (colorless) is studied kinetically. The rate of color removal depends on the concentration of reactants, pH, and temperature. The decolorization of MB⁺ is pseudo first order with respect to MB⁺ and SO₃²⁻. The decolorization increases with temperature, in acidic medium, after addition of Fe(II) and Cu(II), but decreases with the addition of Mn (II), Ni(II), Co(II) and Zn(II).

References

- Ganesh R, Boardman GD, Mochelson F (1994) Fate of azo dyes in sludges. Water Res 28: 1367- 1372.
- Yadav A, Neraliya S, Gopesh A (2007) Acute toxicity levels and ethological responses of Channa striatus to fertilizer industrial wastewater. J Environ Biol 28: 159-162.

3. Weber EJ, Adams RL (1995) Electrochemical monitoring of water remediation by metallic iron. *Environ Sci Technol* 29: 113-121.
4. Mathur N, Bhatnagar P (2007) Mutagenicity assessment of textile dyes from Sanganer (Rajasthan). *J Environ Biol* 28: 123-126.
5. Kang SF, Liao CH, Po ST (2000) Decolorization of textile wastewater by photo-fenton oxidation technology. *Chemosphere* 41: 1287-1294.
6. Hideaki A (2001) Water-based ball-point pen ink composition. US Patent 6261352.
7. Saquib M, Abu Tariq M, Haque MM, Muneer M (2008) Photocatalytic degradation of disperse blue 1 using UV/TiO₂/H₂O₂ process. *J Environ Manage* 88: 300-306.
8. Jain R, Shrivastava M (2008) Photocatalytic removal of hazardous dye cyanosine from industrial waste using titanium dioxide. *J Hazard Mater* 152: 216-220.
9. El-Sharkawy EA, Soliman AY, Al-Amer KM (2007) Comparative study for the removal of methylene blue via adsorption and photocatalytic degradation. *J Colloid Interface Sci* 310: 498-508.
10. Lang AR (2009) *Dyes and pigments: new research*, Nova Science, New York, 44-45.
11. Olajire AA, Giwa AA, Bello IA (2013) Adsorptive removal of methylene blue dye by melon husk: kinetics and isothermal studies. *Pak J Sci Ind Res* 56: 151-164.
12. Olajire AA, Giwa AA, Bello IA (2014) Competitive adsorption of dye species from aqueous solution onto melon husk in single and ternary dye systems. *Int J Environ Sci and Tech* (in press).
13. Giwa AA, Bello IA (2013) Removal of basic dye from aqueous solution by adsorption on melon husk in binary and ternary systems. *Chemical and Process Engineering Research* 13: 51 – 68.
14. Rafatullah M, Sulaiman O, Hashim R, Ahmad A (2010) Adsorption of methylene blue on low-cost adsorbents: a review. *J Hazard Mater* 177: 70-80.
15. El-Jamal MM, Ncibi MC (2012) Biosorption of methylene blue by chaetophora elegans algae: kinetics, equilibrium and thermodynamic studies. *Acta Chim Slov* 59: 24-31.
16. Abu Ghalwa NM1, Zaggout FR (2006) Electrodegradation of methylene blue dye in water and wastewater using lead oxide/titanium modified electrode. *J Environ Sci Health A Tox Hazard Subst Environ Eng* 41: 2271-2282.
17. Panizza M, Barbucci A, Ricotti R and Cerisola G (2006) Electrochemical degradation of methylene blue. *Sep Purif Technol* 54: 382-387.
18. Pant D, Singh A, Satyawali Y, Gupta RK (2008) Effect of carbon and nitrogen source amendment on synthetic dyes decolorizing efficiency of white-rot fungus, *Phanerochaete chrysosporium*. *J Environ Biol* 29: 79-84.
19. Laowansiri S, Vinitnantharath S, Chairprasert P, Ha SR (2008) Anaerobic degradation kinetics of reactive dye with different carbon sources. *J Environ Biol* 29: 309-314.
20. Entezari MH, Sharif Al-Hoseini Z (2007) Sono-sorption as a new method for the removal of methylene blue from aqueous solution. *Ultrason Sonochem* 14: 599-604.
21. Lachheb H, Puzenat E, Houa A, Ksibi M, Elaloui E, et al. (2002) Photocatalytic degradation of various types of dyes (Alizarin S, Crocein Orange G, Methyl Red, Congo Red, Methylene Blue) in water by UV-irradiated titania. *J Applied Catalysis B: Environmental* 39: 75-90.
22. Impert O, Katafias A, Kita P, Mills A, Pietkiewicz-Graczyk A, et al. (2003) Kinetics and mechanism of a fast Leuco-methylene blue oxidation by copper (II)-halide species in acidic aqueous media. *Dalton Trans* 348- 353.
23. Katafias A, Koter S (2009) Autoxidation of Leuco-methylene blue-The role of the methylene blue radicals and reactive oxygen species. *Polish J Chem* 83: 1139 – 1146.
24. Pande S, Ghosh SK, Nath S, Praharaj S, Jana S, et al. (2006) Reduction of methylene blue by thiocyanate: kinetic and thermodynamic aspects. *J Colloid Interface Sci* 299: 421-427.
25. Edwards JC (2000) Investigation of Color Removal by Chemical Oxidation for Three Reactive Textile Dyes and Spent Textile Dye Wastewater, MS of Science in Environmental Science and Engineering. Blacksburg, Virginia.
26. Salem IA, El-Maazawi MS (2000) Kinetics and mechanism of color removal of methylene blue with hydrogen peroxide catalyzed by some supported alumina surfaces. *Chemosphere* 41: 1173-1180.
27. Banat F, Al Ashesh S, Al Rawashedah M, Nusair M (2005) Photodegradation of methylene blue by the UV/H₂O₂ and UV/acetone oxidation processes. *Desalination* 181: 225 – 232.
28. Jian-xiao LV, Ying C, Guo-hong X, Ling-yun Z, Su-Fen W (2011) Decolorization of methylene blue simulated wastewater using UV-H₂O₂ combined system. *J of Reuse and Desalination* 1: 45 – 51.
29. Mowry S, Ogren PJ (1999) Kinetics of methylene blue reduction by ascorbic acid. *J Chem Edu* 76: 970 – 973.
30. Pietkiewicz-Graczyk A, Impert O, Katafias A, Kita P (2003) Reactivity of two protolytic forms of methylene blue on reaction with ascorbic acid. *Polish J Chem* 77: 475 – 480.
31. Khan MN, Sarwar A (2001) The influence of transition metal ions on the kinetics of ascorbic acid oxidation by methylene blue in strongly acidic media. *Turk J Chem* 25: 433 – 440.
32. Tewari BB (2005) Dehydrogenation studies of ascorbic acid with methylene blue in the presence of copper hexacyanoferrate (II) complex and light. *Bull Chemists and Technologists of Macedonia* 24: 109 – 115.
33. Katafias A, Kita P, Wrzeszcz G (2006) Kinetics of the methylene blue oxidation by cerium (IV) in sulphuric acid solutions. *Trans Metal Chem* 32: 31 – 37.
34. Gemeay AH, El-Ghrabawy GR, Zaki AB (2007) Kinetics of the oxidative decolorization of Reactive Blue-19 by acidic bromate in homogeneous and heterogeneous media. *Dyes and Pigments* 73: 90 -97.
35. Zhu X1, Zhang Y (2008) Inhibition kinetic determination of trace amount of iodide by the spectrophotometric method with rhodamine B. *Spectrochim Acta A Mol Biomol Spectrosc* 70: 510-513.
36. Mohammed Y, Etonihu AC, Tsaku VA (2011) Hexamethylpararosalinine (Crystal Violet) Oxidation by Chlorate Ions in Aqueous Acidic Medium: Kinetic Approach to the mechanism of reaction. *Trakia J of Sci* 9: 1-7.
37. Kusvuran E1, Gulnaz O, Samil A, Yildirim O (2011) Decolorization of malachite green, decolorization kinetics and stoichiometry of ozone-malachite green and removal of antibacterial activity with ozonation processes. *J Hazard Mater* 186: 133-143.
38. Cuiqing B, Xianfeng X, Wenqi G, Dexin F, Mo X, et al. (2011) Removal of Rhodamine B by ozone-based advanced oxidation process. *Desalination* 278: 84-90.
39. Deng KJ, Huang F, Wang DY, Peng ZH, Zhou YH (2004) Green Oxygenation Degradation of Rhodamine B by Using Activated Molecule Oxygen. *Chinese Chem Letters* 15: 1223-1226.
40. Fan HJ, Huang ST, Chung WH, Jan JL, Lin WY, et al. (2009) Degradation pathways of crystal violet by Fenton and Fenton-like systems: condition optimization and intermediate separation and identification. *J Hazard Mater* 171: 1032-1044.
41. Hameed BH, Lee TW (2009) Degradation of malachite green in aqueous solution by Fenton process. *J Hazard Mater* 164: 468-472.
42. Bouasla C, Ismail F, Samar ME (2012) Effects of operator parameters, anions and cations on the degradation of AY99 in an aqueous solution using Fenton's reagent. Optimization and kinetics study. *International Journal of Industrial Chemistry* 3; 15 – 26.
43. Kumar A, Paliwal M, Ameta R, Ameta S (2008) Photochemical treatment of rhodamine-B waste-water by photo-Fenton reagent, *Indian J of Chem Technol* 15: 7-11.
44. Mcheik AH, El Jamal MM (2013) Kinetic study of the discoloration of rhodamine B with persulfate, iron activation. *Journal of Chemical Technology and Metallurgy* 48: 357-365.
45. Mills A, Wang J (1999) Photobleaching of methylene blue sensitized by TiO₂: an ambiguous system. *J Photochem Photobiol A* 127: 123-134.
46. Randorn C, Wongnawab S, Boonsin P (2004) Bleaching of methylene blue by hydrated titanium dioxide. *Sci Asia* 30: 149-156.
47. Plater MJ (2003) A degradation product of methylene blue. *ARKIVOC* (i): 37 – 42.
48. Resch P, Field RJ, Schneider FW, Burger M (1989) Reduction of ethylene blue by sulphide ion in the presence and absence of oxygen: simulation of the methylene blue-O₂-HS-CSTR Oscillations. *J Phys Chem* 93: 8181 – 8186.

49. Azmat R (2004) Kinetics of methylene blue with organic reduction, 2004. Thesis of the University of Karachi, 75270, Pakistan.
50. Dilgin Y, NiÅYli G (2005) Fluorimetric determination of ascorbic acid in vitamin C tablets using methylene blue. *Chem Pharm Bull (Tokyo)* 53: 1251-1254.
51. Raffia A, Fahim U (2010) Photoredox reaction of methylene blue and lactose in alcoholic buffered solution. *J Appl Chem Res* 13: 72-84.
52. Olga I, Anna K, Przemyslaw K, Adrew M, Aleksandra V, et al. (2002) Kinetics and mechanisms of a fast leuco- methylene blue oxidation by copper II-halide species in acidic aqueous media. *Dalton Trans* 348-353.
53. Abo-Farha SA (2010) Photocatalytic degradation of monoazo and diazo dyes in wastewater on nanometer-sized TiO₂. *Researcher* 2: 1-20.
54. Behnajady MA, Modirshahla N, Ghanbary F (2007) A kinetic model for the decolorization of C.I. Acid Yellow 23 by Fenton process. *J Hazard Mater* 148: 98-102.
55. Sun JH, Sun SP, Wang GL, Qiao LP (2007) Degradation of azo dye Amido black 10B in aqueous solution by Fenton oxidation process. *Dyes and Pigments* 74: 647-652.
56. Malik PK, Sk S (2003) Oxidation of direct dyes with hydrogen peroxide using ferrous ion as catalyst. *Sep Purif Technol* 31: 241-250.
57. Hassan MY, Ahmed F (1995) Role of anionic micelles in the oxidation of DL-Leucine by acid permanganese. *A Kinetic Study Communi* 18: 128-132.
58. Rangelova K-, Mason RP (2009) New insights into the detection of sulfur trioxide anion radical by spin trapping: radical trapping versus nucleophilic addition. *Free Radic Biol Med* 47: 128-134.
59. Rangelova K, Rice AB, Khajo A, Triquigneaux M, Garantziotis S, et al. (2012) Formation of reactive sulfite-derived free radicals by the activation of human neutrophils: an ESR study. *Free Radic Biol Med* 52: 1264-1271.
60. Zhang L, Chen L, Xiao M, Zhang L, Wu F, et al. (2013) Enhanced decolorization of orange II solutions by the Fe (II) – sulphite system under xenon lamp irradiation. *Ind Eng Chem Res* 52: 10089-10094.
61. Hayon E, Treinin A, Wilf J (1972) Electronic spectra, photochemistry, and autoxidation mechanism of the sulfite-bisulfite-pyrosulfite systems. SO₂-, SO₃-, SO₄-, and SO₅- radicals. *J Am Chem Soc* 94: 47-57.
62. Neta P, Huie RE (1985) Free-radical chemistry of sulfite. *Environ Health Perspect* 64: 209-217.
63. McCord JM, Fridovich I (1969) The utility of superoxide dismutase in studying free radical reactions. I. Radicals generated by the interaction of sulfite, dimethyl sulfoxide, and oxygen. *J Biol Chem* 244: 6056-6063.
64. Shi X (1994) Generation of SO₃- and OH radicals in SO₃(2-) reactions with inorganic environmental pollutants and its implications to SO₃(2-) toxicity. *J Inorg Biochem* 56: 155-165.
65. Eyring H (1935) The activation complex in chemical reactions. *J Chem Phys* 3: 107.
66. Iyun JF, Ayoko GA, Lawal HM (1992) Kinetics and mechanism of the oxidation of iodide by diaquotetrakis(2,2'-bipyridine)-μ-oxodiruthenium(II) ion in acid medium. *Trans Met Chem* 17: 63-65.
67. Iyun JF, Ayoko GA, Lohdip YN (1992) The kinetics and mechanism of the oxidation of diaquotetrakis(2,2'-bipyridine)-oxodiruthenium(III) ion by bromate in aqueous perchloric acid. *Polyhedron* 11: 2389-2394.